2012

Self-optimizing Control of Cooling Tower for Efficient Operation of Chilled Water Systems

Xiao Li
randy131@gmail.com

Yaoyu Li

John E. Seem

Pengfei Li

Self-optimizing Control of Cooling Tower for Efficient Operation of Chilled Water Systems

Xiao Li[1]*, Yaoyu Li[2], John E. Seem[3], Pengfei Li[4]

[1]Department of Mechanical Engineering, University of Wisconsin-Milwaukee, Milwaukee, WI, USA
randy131@gmail.com
[2]Department of Mechanical Engineering, University of Texas at Dallas, Richardson, TX, USA
yaoyu.li@utdallas.edu
[3]Building Efficiency Research Group, Johnson controls, Inc., Milwaukee, WI, USA
john.seem@gmail.com
[4]United Technologies Research Center, East Hartford, CT, USA
lip1@utrc.utc.com
* Corresponding Author

ABSTRACT

The chilled-water systems, mainly consisting of electric chillers and cooling towers, are crucial for the ventilating and air conditioning systems in commercial buildings. Energy efficient operation of such systems is thus important for the energy saving of commercial buildings. This paper presents an extremum seeking control (ESC) scheme for energy efficient operation of the chilled-water system, and presents a Modelica based dynamic simulation model for demonstrating the effectiveness of the proposed control strategy. The simulated plant consists of a water-cooled screw chiller and a mechanical-draft counter-flow wet cooling tower. The ESC scheme takes the total power consumption of the chiller compressor and the tower fan as feedback, and uses the fan speed setting as the control input. The inner-loop controllers for the chiller operation include two proportional-integral (PI) control loops for regulating the evaporator superheat and the chilled water temperature. Simulation was conducted on the dynamic simulation model of the whole plant including the screw chiller and the cooling tower for different scenarios. The simulation results demonstrated the effectiveness of the proposed ESC strategy in searching for the optimal tower fan speed set-point under tested circumstances, and the potential for energy saving is also evaluated.

1. INTRODUCTION

About 40% of U. S. primary energy consumption comes from the building sector, including both commercial and residential buildings (U. S. Department of Energy 2010). The heating, ventilation and air conditioning (HVAC) systems account for about 32% of the energy used in the commercial buildings (Sane et al. 2006). Figure 1(a) shows the schematic of a typical chilled-water ventilation and air-conditioning system for commercial buildings, which consists of three main components: air handling unit, chiller and cooling tower. The power consumption of such system is mainly due to the chiller compressor and the cooling tower fan. Due to the significant variations in ambient, load and equipment conditions, developing proper control strategy is critical for efficient operation of chilled-water systems.

Optimization and control techniques have been well investigated for the chilled-water system in the past (Kaya and Sommer 1984; Braun and Diderrich 1990; Lu et al. 2004; Yao et al. 2004; Sun and Reddy 2005; Sane et al. 2006; Tyagi et al. 2006; Ma et al. 2008; Liu and Chuah 2011). Kaya and Sommer (1984) presented a supervisory control strategy for chillers by finding the optimal temperature difference between the chilled water supply and return temperatures due to the trade-off between the energy cost by pumping and refrigeration. Yao et al. (2004) presented an optimal operation of chilled-water system by performing a constrained optimization based on the empirical models of the system components, and an index of *system coefficient of performance* (SCOP) is proposed to evaluate the energy saving benefit. Liu and Chuah (2011) proposed an hourly regulated optimal control scheme using the approach temperature control (the difference between the ambient wet bulb temperature and the condenser water temperature) instead of directly finding the optimal condenser water temperature, a regression function is used to predict the optimal approach temperature. In particular, Braun and Diderrich (1990) studied the coupling between the power consumption of chiller compressor and cooling tower fan. As shown in Fig. 2(a), they demonstrated that the tower fan power increases with the relative tower airflow, while the chiller power decreases. As net effect, the total power consumption shows a global minimum, as shown in Fig. 2(a). The total power curve also demonstrates a strong convex characteristics, which would facilitate the use of any gradient search type of optimization methods. Then, the authors proposed an open-loop control scheme to search for the nearly optimal fractional tower airflow based on the parameter estimation of the design characteristics of the chiller and cooling tower. Similar to this study, most existing methods to the control and optimization of the chilled-water systems have been based on nominal/empirical models. In practice, due to the unknown environment changes and the hard estimated system degradation, such models may often be inaccurate. Therefore, real-time optimization of set-point tracking without exact system knowledge is more desirable for operations of the chiller plant. The extremum seeking control (ESC), as a major class of self-optimizing strategies, has recently drawn significant attention for the HVAC applications.

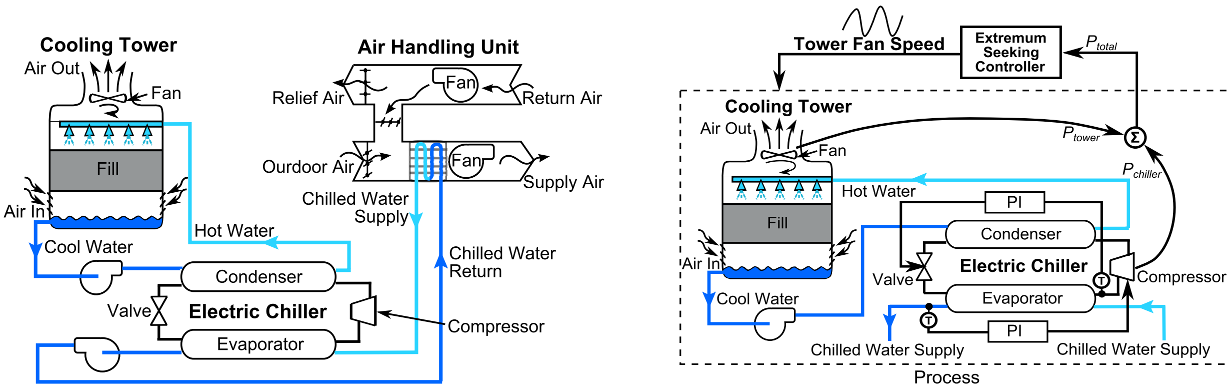

(a) (b)

Figure 1: (a) Schematic of a typical chilled-water ventilation and air-conditioning system. (b) Basic system diagram of ESC working on chiller-tower system.

The objective of ESC is to search for the optimal input in real time in a nearly model-free fashion (Ariyur and Krstic 2003; Krstic 2000; Krstic and Wang 2000). P. Li et al. (2010) presented an ESC scheme for efficient operation of the air-side economizer. For chilled-water systems, application of ESC has been recently investigated (Sane et al. 2006; Tyagi et al. 2006). Tyagi et al. (2006) presented a work with golden-section search as their extremum seeking solution for determining the optimal condenser supply water temperature based on an oracle function. Such scheme may lead to long searching time in practice since every step of search needs to wait for the system transient to settle. For the same problem, Sane et al. (2006) described a dither ESC solution, where again the condenser supply temperature is used as the control input. Simulation results were shown without mentioning the details about the simulation platform. As the dither ESC is a dynamic scheme of gradient search, a key aspect of its design is to compensate for the input and output dynamics. An ESC design of such may not be sufficient without simulation on a dynamic model of cooling tower and chiller. Also, the control input adopted in (Sane et al. 2006) and (Tyagi et al. 2006), i.e. the condenser supply water temperature, is not a variable that can be directly manipulated in practice. Some inner loop control of the cooling tower must be implemented. In addition, its operation contains another uncertainty, i.e. the reliability of the associated temperature sensor.

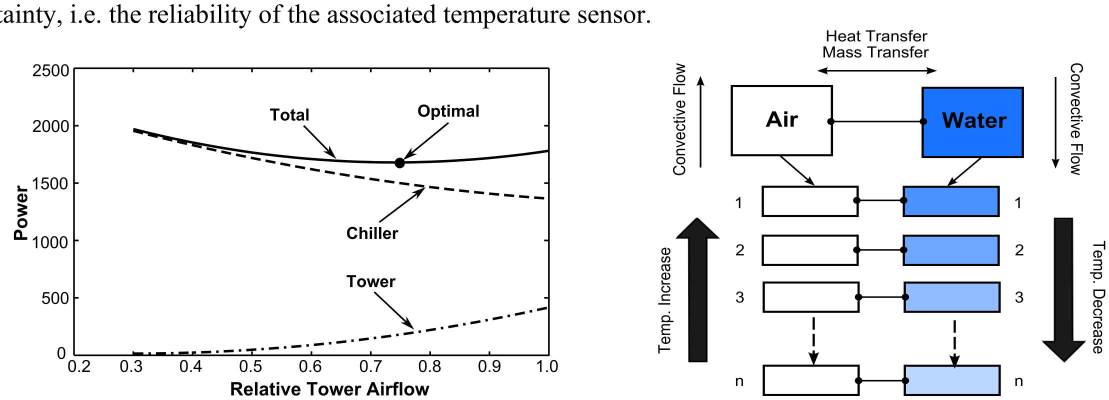

(a) (b)

Figure 2: (a) Tradeoff between energy consumption of chiller and cooling tower (reproduction of Fig. 2 in Braun and Diderrich (1990)). (b) Illustration of control volumes for tower modeling.

With these concerns considered, this study approaches to the ESC based chilled-water system control problem with two different perspectives. First, a Modelica (Modelica 2012) based dynamic simulation model platform is developed for the cooling tower in Dymola (Dynasim 2012). Second, the cooling tower fan speed, instead of the condenser supply water temperature, is used the input for the ESC control design. With the typical variable-speed drive (VSD) equipped for the cooling towers nowadays, setting the VSD frequency or the motor speed is direct and simple. No cost or uncertainty is needed for the temperature sensor than otherwise. With constant condenser water flow rate assumed, the total power consumption of the chiller compressor and the cooling tower fan is used as the performance index for feedback. In particular, a screw chiller is chosen for the simulation plant model, which would not affect the generality of the results for plants with other types of chillers. The proposed ESC framework is illustrated in the schematic in Fig. 1(b). The reminder of this paper is structured as follows. The dynamic models of cooling tower and screw chiller used for ESC controller design and simulation validation are presented in next section. Then the design framework of ESC is briefly reviewed. Finally, the ESC controller is designed based on the estimated system input dynamics and the effectiveness of the ESC algorithm is validated by simulation results.

2. DYNAMIC MODELING OF CHILLER-TOWER SYSTEM

The dynamic model of chiller-tower system is developed with Dymola 2012 FD1 (Dynasim 2012), TIL Library 2.0.1 and TIL Media Library 2.0.4 (TLK-Thermo 2012). The cooling tower model follows our recent work in (Li et al. 2010), which is a modification of the work by Braun et al. (1989). The screw compressor modeling follows the work by Zhang et al. (2009), while the condenser, evaporator and expansion device models are based on the work of Li et al. (2012). For other components, such as fan, pump, tank and valve, we have adopted those avalilable in the TIL Library 2.0.1. Two control loops have been implemented for the screw chiller model: one for the evaporator superheat control and the other for the chilled water temperature regulation. All the controllers and plant model are integrated into simulation platform.

2.1 Dynamic Modeling of Cooling Tower

Cooling towers reject heat via evaporative cooling (Kröger 2004). Hot water is sprayed from the top, and air is drawn from the bottom by tower fan. As water falls through the fill, water temperature decreases due to evaporative cooling. In this study, finite volume method is used to model the one-dimensional heat and mass transfer process. The dynamic balances of mass and energy are established for both the water and air sides, with control volumes shown in Fig. 2(b). The transient mass and energy storage is treated at the water side but neglected at the air side.

Following (Li et al. 2010), for the i^{th} water-side control volume, the energy balance is established as

$$m_{w,i} \cdot c_{p,w,i} \cdot \frac{dT_{w,i}}{dt} = \dot{m}_{w,in,i}\left(h_{w,in,i} - h_{w,i}\right) - \dot{m}_{w,out,i}\left(h_{w,out,i} - h_{w,i}\right) - \dot{q}_i \tag{1}$$

where $m_{w,i}$ is the mass of water stored in the cell, $c_{p,w,i}$ is the specific heat of water (which can be determined by the local water temperature $T_{w,i}$), $\dot{m}_{w,in,i}$ and $\dot{m}_{w,out,i}$ are the mass flow rates for the inlet and outlet water flow, respectively, $h_{w,in,i}$ and $h_{w,out,i}$ are the specific enthalpy of the inlet and outlet water flow, respectively, and $h_{w,i}$ is the specific enthalpy of water in the cell. $\dot{q}_i$ is the heat flow transferred to the neighbored (also the i^{th}) moist-air cell, which includes both the sensible heat flow and the latent heat flow due to evaporation.

For the mass balance of the same water-side control volume, cell volume V_{cell} is assumed as constant, while water density $\rho_{w,i}$ may change with evaporation and temperature change in the cell. The dynamic mass balance of the i^{th} water cell is given by (Li et al. 2010):

$$\frac{d\left(V_{effective}\rho_{w,i}\right)}{dt} = \frac{dV_{effective}}{dt}\rho_{w,i} + V_{effective}\frac{d\rho_{w,i}}{dt} = \dot{m}_{w,in,i} - \dot{m}_{w,out,i} - \dot{m}_{evap,i} \tag{2}$$

where $\dot{m}_{evap,i}$ is the vapor mass transfer flow rate into the moist air side. $V_{effective}$ is the water droplet volume in the cell. The ratio of water droplet per unit volume of the tower is around the level of 0.001(Bernier 1995). $V_{effective}$ can be obtained by (Bernier 1995): $V_{effective} = V_{cell}\dot{m}_{w,in} / \rho_{w,i}A_T v_w$. The velocity of water droplets under free fall (no packing) v_w is assumed constant. A_T is the cross-sectional area of the tower. Taking time derivative of the equation of $V_{effective}$ yields

$$\frac{dV_{effective}}{dt}\rho_{w,i} = \frac{V_{cell}}{A_T v_w}\frac{d\dot{m}_{w,in}}{dt} \tag{3}$$

Equation (3) reveals that if $\dot{m}_{w,in}$ does not vary much, $V_{effective}$ can be assumed as constant; otherwise, the gradient of $\dot{m}_{w,in}$ is needed to account for the change of $V_{effective}$.

The time derivative of density ρ can be expressed as function of pressure P and specific enthalpy h (Richter 2008):

$$\frac{d\rho}{dt}=\left(\frac{\partial\rho}{\partial P}\right)_h\frac{dP}{dt}+\left(\frac{\partial\rho}{\partial h}\right)_P\frac{dh}{dt} \tag{4}$$

As the cell pressure is approximately constant for the cooling tower operation, Eq. (4) can be simplified as

$$\frac{d\rho}{dt}=-\frac{\beta\rho}{c_{pw}}\frac{dh}{dt}=-\beta\rho\frac{dT}{dt} \tag{5}$$

where $\beta=-\frac{1}{\rho}\left(\frac{\partial\rho}{\partial T}\right)_P$ is the isobaric coefficient of expansion and c_{pw} is the specific heat capacity at constant pressure. Substituting Eq. (5) into Eq. (2) leads to the mass balance of the i^{th} water cell:

$$\dot{m}_{w,in,i}-\dot{m}_{w,out,i}-\dot{m}_{evap,i}=-V_{effective}\beta_{w,i}\rho_{w,i}\frac{dT_{w,i}}{dt}+\frac{V_{cell}}{A_T v_w}\frac{d\dot{m}_{w,in}}{dt} \tag{6}$$

where $\beta_{w,i}$ and $\rho_{w,i}$ can be determined by the local water temperature.

At the air side, the steady-state relations were derived following the detailed analysis model by Braun et al. (1989)

$$\dot{H}_{a,in,i}-\dot{H}_{a,out,i}+\dot{q}_i=0 \tag{7}$$

$$\dot{q}_i=\dot{q}_{sen,i}+\dot{q}_{lat,i} \tag{8}$$

The sensible and latent heat flow rates can be determined by

$$\dot{q}_{sen,i}=h_{C,i}A_V V_{cell}\left(T_{w,i}-T_{a,i}\right) \tag{9a}$$

$$\dot{q}_{lat,i}=h_{f,g,i}\cdot\dot{m}_{evap,i}=h_{f,g,i}\cdot h_{D,i}A_V V_{cell}\left(\omega_{s,w,i}-\omega_{a,i}\right) \tag{9b}$$

where $h_{C,i}$ is the local heat transfer coefficient, A_V is the surface area of water droplets per unit volume, $T_{a,i}$ is the local air temperature, $h_{f,g,i}$ is the latent heat of vaporization depending on the local water temperature. $h_{D,i}$ is the local mass transfer coefficient, $\omega_{s,w,i}$ is the saturated-air humidity ratio at the local water temperature, and $\omega_{a,i}$ is the local humidity ratio of the moist air.

The fill is used in most cooling towers, however, it is usually hard to predict its heat rejection performance analytically because of the difficulty in evaluating the contact time and the surface area between the air and the water through the fill (Bernier 1994). The fouling in the packing materials may result in a reduction in the overall effectiveness of the tower and make it even harder to evaluate the fill geometry accurately. Due to the difficulty in getting a general correlations for heat and mass transfer in cooling tower in terms of the physical tower characteristics, the NTU and the Lewis relation Le_f have been used to characterize the heat and mass transfer coefficients for specific tower designs (Braun et al. 1989).

The mass transfer coefficient can be derived by using the overall NTU for mass transfer, i.e.

$$NTU=\frac{h_D A_V V_T}{\dot{m}_{a,in}} \tag{10}$$

where V_T is the total tower volume and $\dot{m}_{a,in}$ is the inlet-air flow rate. The mass transfer coefficient can thus be determined with

$$h_D A_V=\frac{NTU\cdot\dot{m}_{a,in}}{V_T} \tag{11}$$

which varies with the tower geometry, NTU and air inlet flow rate. The heat transfer coefficient is determined by

$$h_{C,i}A_V=\frac{Le_f\cdot NTU\cdot c_{pm,i}\cdot\dot{m}_{a,in}}{V_T} \tag{12}$$

where Le_f is defined as $Le_f=h_C/h_D c_{pm,i}$ and the local specific heat of moist air $c_{pm,i}$ is determined by $c_{pm,i}=c_{pa,i}+\omega_{a,i}c_{pv,i}$. $c_{pa,i}$ is the local specific heat of dry air and $c_{pv,i}$ is the local specific heat of water vapor (Braun 1988). $h_{C,i}$ may change with the local value of Le_f and $c_{pm,i}$.

The Merkel's Number Me_M can be related to the mass transfer coefficient by (ASHRAE 2008):

$$Me_M=\frac{h_D A_V V_T}{\dot{m}_{w,in}}=c\left(\frac{\dot{m}_{w,in}}{\dot{m}_{a,in}}\right)^n \tag{13}$$

where $\dot{m}_{w,in}$ is the water inlet flow rate of cooling tower, c and n are empirical constants specific to a particular tower design. Kröger (2004) developed a methodology to obtaining the Merkel's number from experimental data with empirical equations of thermal properties. Multiplying both sides of Eq. (13) by $\dot{m}_{w,in} / \dot{m}_{a,in}$ leads to

$$NTU = c\left(\frac{\dot{m}_{w,in}}{\dot{m}_{a,in}}\right)^{n+1} \tag{14}$$

where coefficients c and n can be fitted from the performance measurements for a specific tower on a log-log plot (Braun et al. 1989). The Lewis relation has been discussed in literature. Poppe and Rogener (1991) cited the definition of the Lewis relation according to Bosnjakovic (1965), i.e.

$$Le_f = Le^{2/3}\left[\left(\frac{\omega_{s,w}+d}{\omega_a+d}-1\right)/\ln\left(\frac{\omega_{s,w}+d}{\omega_a+d}\right)\right] \tag{15}$$

where Le is the Lewis number, assumed as a constant of 0.865. d is the ratio of the molecular weight of water to the molecular weight of air, which is a constant of 0.622. Grange (1994) and Bourillot (1983) claimed that for a wet cooling tower, Eq. (15) is approximately 0.92. Kloppers and Kröger (2005) stated that, if the ambient air is very humid, variation of the Lewis relation has little influence on the water outlet temperature, and neither on the heat rejected from the cooling tower; while for dry conditions, variation of the Lewis relation can lead to significantly different results. It was also suggested that the equation by Bosnjakovic (1965) should be used, and a numerical value of 0.92 be preferred when fill performance test data is insufficient to accurately predict the Lewis relation of a particular fill. The cooling tower fan model and the collection basin model follows the commercial packages from TIL Library (TLK-Thermo 2012). Detailed description of the models could be found in our work in (Li et al. 2010).

3. MODELING OF SCREW CHILLER AND INNER LOOP CONTROL DESIGN

3.1 Screw Compressor

The dynamics of screw compressor is much faster than that of the entire chiller cycle. For this study, a transient model of screw compressor is not necessary. Instead, the polytropic static compression model developed by Zhang et al. (2009) is adopted

$$\dot{m}_{c,in} = s_{comp}\rho_{c,in}n_c V_{c,max}\eta_{c,v} \tag{16}$$

$$P_{c,out} = P_{c,in}\left(\rho_{c,out} / \rho_{c,in}\right)^{\gamma_c} \tag{17}$$

where $\dot{m}_{c,in}$ is the refrigerant mass flow rate at compressor inlet, and $s_{comp}\in[0, 1]$ is the slide-valve control, which determines the compressor load. s_{comp} is used to regulate the chilled water temperature. $\rho_{c,in}$ and $\rho_{c,out}$ are the refrigerant densities at the compressor inlet and outlet, respectively. n_c is the compressor speed. $V_{c,max}$ is the theoretical compressor volume with full load condition. $P_{c,in}$ and $P_{c,out}$ are the compressor inlet and outlet pressures, respectively. γ_c is the ratio of specific heats in the compressor, and $\eta_{c,v}$ is the volumetric efficiency. Volumetric efficiency could be obtained from the pressure volume curve (Hanlon 2001). ASHARE (2008) suggests linear pressure-volume characteristic for the pressure ratio raning from 2 to 9, for both twin-screw and single screw compressors. The volumetric efficiency is determined as

$$\eta_{c,v} = 0.95 - 0.0125\cdot\left(\frac{P_{c,out}}{P_{c,in}}\right) \tag{18}$$

following Fu et al. (2002). The electrical power consumed by the compressor is

$$W_{c,elec} = \frac{\dot{m}_{c,out}\cdot\left(h_{c,out}-h_{c,in}\right)}{\eta_{c,a}\eta_{c,mo}\eta_{c,me}} \tag{19}$$

where $\dot{m}_{c,out}$ is the refrigerant mass flow rate at the compressor outlet. $h_{c,in}$ and $h_{c,out}$ are the inlet and outlet specific enthalpies, respectively. $\eta_{c,a}$, $\eta_{c,mo}$ and $\eta_{c,me}$ are the adiabatic efficiency, motor efficiency and mechanical efficiency, chosen as 0.8, 0.85 and 0.95, respectively (Fu et al. 2002).

3.2 Condenser, Evaporator and Expansion Valve

The shell-and-tube heat exchanger models of condenser and evaporator in the screw chiller follow the work by Li et al. (2012). Both exchangers are of the counter-flow type with in-tube water flow. Based upon the adoption of concentric heat exchanger, the shell-side heat transfer area is calculated based on the water-tube outer surface area and the surface enhancement factor. The finite volume method is applied for both the water and the refrigerant sides. The heat transfer is considered between each pair of the cells. The mass and energy balances are set for each cell (both refrigerant and water side).

The thermal expansion valve (TXV) model in (Richter 2008) is adopted, which assumes a quadratic relation between the mass flow rate and the pressure difference across the valve. The effective flow area is set as an external input, which can be used to regulate the evaporator superheat for the chiller. No transient mass storage is assumed for the TXV, and an isenthalpic throttling process is considered.

3.3 Two Inner-Loop PI Controls

The superheat control is important for chiller operation. In the evaporator, liquid refrigerant has a much higher heat transfer coefficient than the vaporized refrigerant. The two-phase flow is desired to maximize the cooling capacity of the system. Meanwhile, if not all the liquid refrigerant gets vaporized before entering the compressor, the remained liquid will damage the compressor. So the evaporator superheat must be maintained to ensure both the safety and the efficiency (Elliott et al. 2009). Also, as required by the air handling unit operation, the chilled water temperature is expected to be maintained around a setpoint (ASHARE 2008). To satify these two needs, for the chiller-tower plant simulated, two inner-loop PI controllers are implemented to regulate superheat and chilled water temperature by tuning the thermal expansion valve's effective flow area (A_{TXV}) and the compressor slide-valve opening (s_{comp}), respectively. The schematic of the chiller-tower system with both ESC controller and inner loop PI controllers is shown in Fig. 3. The set points of the evaporator super heat and chilled water temperature are assumed as 5°C and 7°C, respectively.

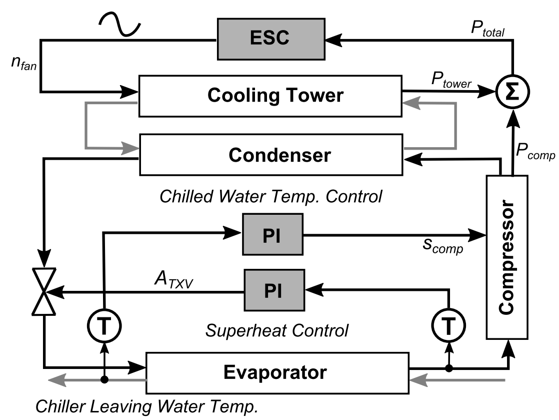

Figure 3: Illustration of chiller-tower system inner loop superheat and chilled water temperature control.

4. BRIEF REVIEW OF EXTREMUM SEEKING CONTROL

The ESC is to find the optimal input $u_{opt}(t)$ in real time for a generally unknown and/or time-varying objective function $l(t,u)$ with the online measurement of the objective value to be minimized, i.e. $u_{opt} = \arg\min_{u\in R^m} l(t,u)$ with $u(t)$ as the input vector. Typical ESC designs are based on the assumption of quadratic objection function, which holds for a reasonable neighborhood of the optimum for a general setting of convex nonlinear mapping. A typical dither ESC block diagram is shown in Fig. 4 (Rotea 2000). The transfer function $F_I(s)$ and $F_O(s)$ denote the input dynamics and sensor dynamics, respectively. The output of the objective function y, which may be corrupted by noise n, is assumed to be directly observable for feedback. The demodulation and signals dither are $d_1^T(t) = [\sin(\omega_1 t) \quad \cdots \quad \sin(\omega_m t)]$ and $d_2^T(t) = [a_1 \sin(\omega_1 t + \alpha_1) \quad \cdots \quad a_m \sin(\omega_m t + \alpha_m)]$, respectively, where ω_i and α_i are the frequency and phase angle, respectively. The dithered output signal passes through the high-pass filter $F_{HP}(s)$, multiplied by the demodulating signal $d_1(t)$ and low-pass filtered by $F_{LP}(s)$, resulting in a signal proportional to gradient $\partial l / \partial u(\hat{u})$. An integrator will help to eliminate the gradient when closing the loop. The compensator $K(s)$ can be designed to enhance the transient performance or stability.

The design of a dither ESC method needs to determine several components mentioned above: the dither signal $d(t)$, the high-pass filter $F_{HP}(s)$, the low-pass filter $F_{LP}(s)$ and the compensator $K(s)$. The dither amplitude a needs to be chosen such that it is small enough to avoid large output oscillation while overcoming the noise effect. The dither frequency ω_d could be determined from the estimation of the system input dynamics $F_I(s)$. $F_{HP}(s)$ and $F_{LP}(s)$ need to be designed to locate ω_d in the pass band of $F_{HP}(s)$ and the stop band of $F_{LP}(s)$. The dither phase angle α should be select to satisfy $\theta = \angle F_I(j\omega) + \angle F_{HP}(j\omega) + \alpha \in (-\pi/2, \pi/2)$. A value close to 0 is recommended for θ. For a standard ESC design, the compensator $K(s)$ could be chosen as a constant. A larger gain in $K(s)$ can enhance the convergence rate, but may also amplify the effort caused by noise or unmodeled system dynamics, which may cause unstable conditions.

The ESC method achieves the convergence to the system optimality based on an integral action on the gradient proportional signal extracted by the pair of dither-demodulation signals, high-pass and low-pass filters.

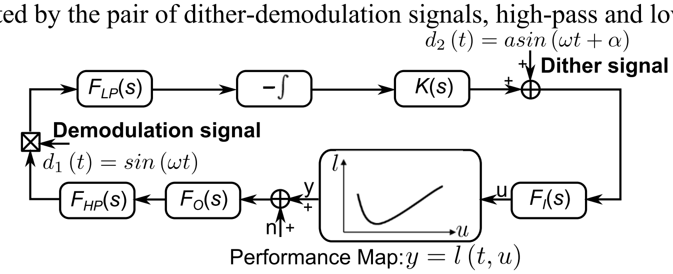

Figure 4: Block diagram of standard dither ESC.

5. SIMULATION STUDY

In this study, the dither ESC framework is applied to the chiller-tower system to minimize the power consumption of the screw chiller and cooling tower fan by tuning the tower fan speed. The input dynamics from the tower fan speed to the total power consumption is estimated based on the system responses of several step changes at both sides of the optimum, as shown in Fig. 5. Then the input dynamics is estimated based the slowest step response to achieve better robustness:

$$\hat{F}_I(s) = \frac{0.0316^2}{s^2 + 2 \cdot 1.06 \cdot 0.0316 s + 0.0316^2} \tag{20}$$

The cutoff frequency of the input dynamics ω_c is about 0.0187 rad/sec. The dither frequency ω_d is selected as 0.0043 rad/sec with $F_{HP}(s) = \frac{s^2}{s^2 + 2 \cdot 0.65 \cdot 0.0025 s + 0.0025^2}$ and $F_{LP}(s) = \frac{0.003^2}{s^2 + 2 \cdot 0.65 \cdot 0.003 s + 0.003^2}$.

The dither amplitude is selected as 7.1 Hz for the VSD input. The dither phase angle is selected as -0.604 radian to ensure $\theta \approx 0$ under the estimated input dynamics of (20).

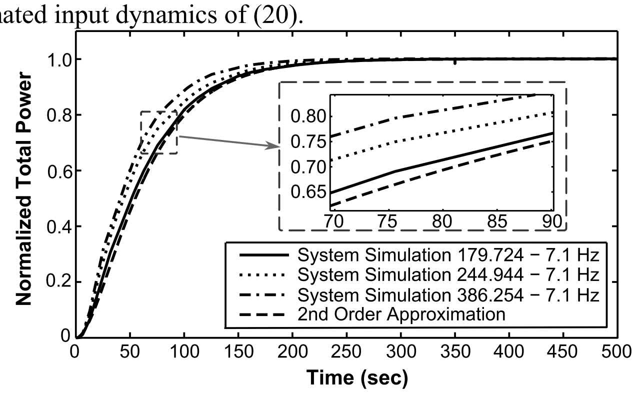

Fig. 5. Comparison of step responses of the full simulation model and the 2nd-order estimate.

The designed ESC is then simulated on the dynamic simulation model of the chiller-tower system that was described earlier. The ESC performance is first tested under a fixed operating condition. The relative humidity and temperature for the cooling-tower inlet air flow are set as 20% and 310 K, respectively. The temperature and mass flow rate of the evaporator inlet water are set as 285.15 K and 13.2 kg/s, respectively. Figure 6(a) shows the static map from cooling tower fan speed to the power consumptions of the chiller compressor and the tower fan, with the optimal fan speed and power consumption estimated as 250.351 Hz and 231174 W, respectively.

The simulation first starts at a fixed fan speed of 200 Hz, and the ESC controller is turned on at t = 5000 sec. As shown in Fig. 6(b), the ESC search results in the averge steady-state fan speed of 256.302 Hz and the total power of 232018 W, respectively, with the 1% settling time of about 11720 sec. Compared to the estimated optimum in the static map, the steady-state error is about 2.37% and 0.37% for the fan speed and the total power, respectively. Notice that Fig. 6(b) shows that the estimated optimal fan speed falls within the range of the input dither. The evaporator superheat and the corresponding valve effective flow area are shown in Fig. 6(c), which validates the effectiveness of the chiller operation through the ESC simulation. Figure 6(d) shows the profiles of the chilled-water temperature and the compressor slide-valve opening. These results show satisfactory inner-loop control performance and reasonable control input profiles, which indicate valid chiller operation through the ESC simulation.

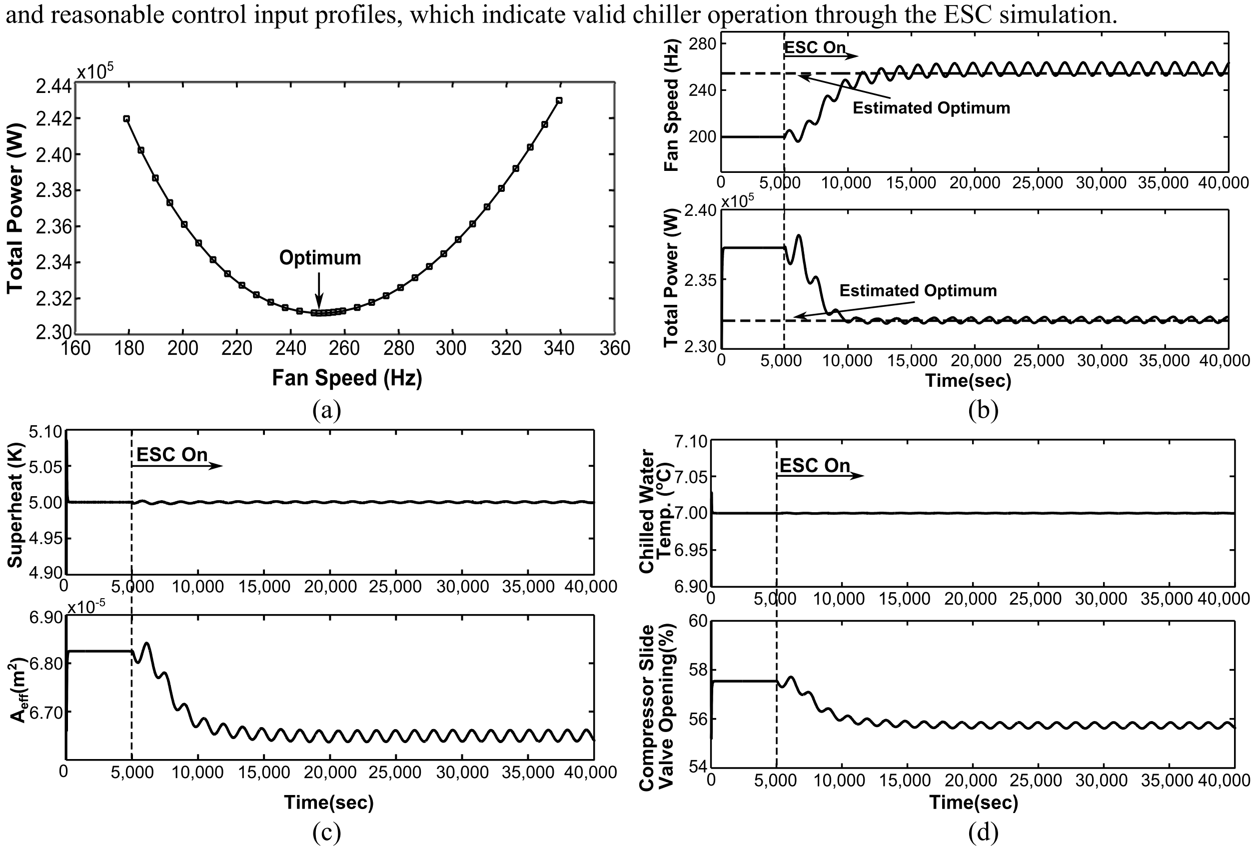

Figure 6: (a) Static map from cooling tower fan speed to total power consumption. (b) Fan speed and power consumption for ESC with fixed operation condition. (c) Superheat control results for ESC with fixed operation condition. (d) Chilled water temperature control for ESC with fixed operation condition.

The ESC controller is then tested with a ramp change in the evaporator inlet water temperature T_{EW} (e.g. due to a load reduction) from 12 °C to 10 °C in 3000 seconds starting from t = 60000 second. The static maps of the two conditions are shown in Fig. 7(a), with the optimal point being (250.351 Hz, 231174 W) for the first condition, and (179.345 Hz , 86527.3 W) for the second condition, respectively. The first condition is the same as the previous case of fixed condition.

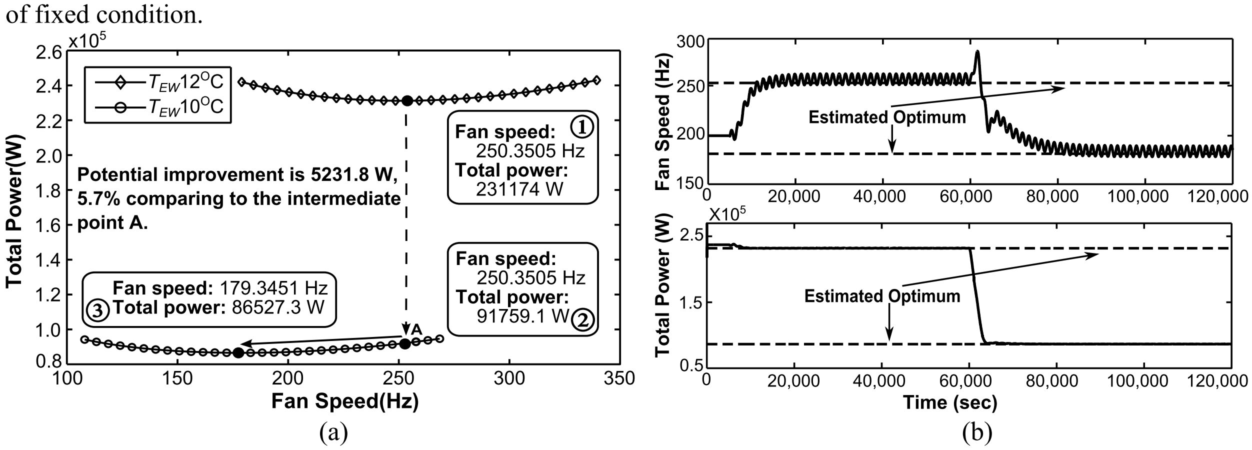

Figure 7: T_{EW} decreased from 12°C to 10°C (a) Static maps. (b) ESC simulation results.

In Fig. 7(b), the ESC searched average steady-state fan speed and power consumption of the second condition are about 182.714 Hz and 86538.4 W, respectively, differing from the estimated optimum by only 1.88% and 0.013%, respectively. The power output settles within ±1% of its steady state in about 13735 second. Also, as marked in Fig. 7(a), if the fan speed remained unchanged during the ramp change, the system would operate at point A, which consumes 91759.1W. Therefore, ESC adapts the system operation with power saving of 5231.8W (5.7%).

Finally the ESC controller is tested with a change in ambient air condition. The tower inlet air temperature drops from 37 °C to 35 °C, and the relative humidity increases from 20% to 80%. The ramp starts at t = 60000 second, and lasts for 3000 seconds. The static maps of the two conditions are shown in Fig. 8(a). The optimal point of the second condition is at 275.089 Hz and 357564 W.

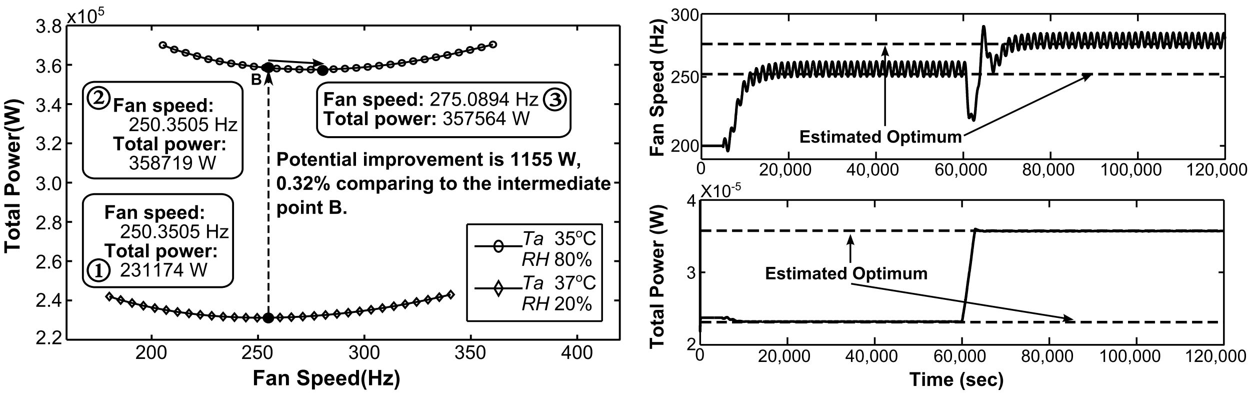

(a) (b)

Figure 8: two inlet air conditions: 37°C and 20% RH versus 35°C and 80% RH (a) Static maps. (b) ESC results.

Figure 8(b) shows that the ESC searched average steady-state fan speed and total power consumption of the second condition are about 279.915 Hz and 357721 W, respectively. The differences are only 1.75% and 0.044%, respectively, compared to the estimated optimal values. Again, the estimated optimal fan speed from the static map falls within the range of input dither. The outputs settle within ±1% of the steady-state values at about 4823 sec. If the fan speed remained unchanged during the ramp change, the operation would be at point B in Fig. 8(a), which indicates that the adaptation of ESC achieves a power saving of 0.32% (1155W).

6. CONCLUSION

This paper presents an ESC based cooling tower control scheme which can minimize the combined power consumption of cooling tower fan and chiller compressor. The ESC strategy is tested on a dynamic simulation model of the chiller-tower system has been developed in Dymola using Modelica. The inner loop controls of superheat and chilled water temperature are implemented, by regulating the valve flow area and the slide-valve opening, respectively. Simulation study was performed for a scenario of fixed condition and then for two scenarios of varying conditions in which ramp changes are introduced to the evaporator inlet water temperature and the ambient air condition, respectively. The ESC searched results show very small steady-state errors compared to the pre-calibrated static maps, with reasonable settling time even under varying conditions. The power saving performance is also evaluated for the simulated examples.

REFERENCES

Ariyur, K. B. and M. Krstić. 2003. *Real-Time Optimization by Extremum-Seeking Control*. John Wiley & Sons, Inc., New York, NY.

ASHRAE. 2008. *ASHARE Handbook - HVAC Systems and Equipment (SI)*. American Society of Heating, Refrigerating, and Air-Conditioning Engineers Inc., Atlanta, GA.

Bernier, M. A. 1994. Cooling Tower Performance: Theory and Experiments. *ASHRAE Trans.* **100**(2): 114-121.

Bernier, M. A. 1995. Thermal Performance of Cooling towers. *ASHRAE Journal* **37**(4): 56-61.

Bosnjakovic, F. 1965. *Technische Thermodinamik*, Theodor Steinkopf, Dresden.

Bourillot, C. 1983. *Numerical Model for Calculating the Performance of an Evaporative Cooling Tower*. Technical Report No. EPRI Report CS-3212-SR.

Braun, J. E. 1988. *Methodologies for the Design and Control of Central Cooling Plants*, University of Wisconsin - Madison. **Ph. D. Thesis**.

Braun, J. E. and G. T. Diderrich. 1990. Near-Optimal Control of Cooling Towers for Chilled Water Systems. *ASHRAE Transactions* **96**(2): 806-816.
Braun, J. E., S. A. Klein and J. W. Michell. 1989. Effectiveness Models for Cooling Towers and Cooling Coils. *ASHRAE Transactions* **95**(2): 164-174.
Dassault Systèmes. 2012. *Dymola: Multi-Engineering Modeling and Simulation*. Online available at: http://www.3ds.com/products/catia/portfolio/dymola.
Elliott, M., Z. Walton, B. Bolding, B. P. Rasmussen. 2009. Superheat Control: A Hybrid Approach. *HVAC&R Research* **15**(6): 1021-1043.
Fu, L., G. Ding, Z. Su and G. Zhao. 2002. Steady-State Simulation of Screw Liquid Chillers. *Applied Thermal Engineering* **22**(15): 1731-1748.
Grange, J. L. 1994. Calculating the Evaporated Water Flow in a Wet Cooling Tower. Paper presented at *the 9th IAHR Cooling Tower and Spraying Pond Symposium*, von Karman Institute, Brussels, Belgium.
Hanlon, P. C. 2001. *Compressor Handbook*. McGraw-Hill, New York City, NY.
Kaya, A. and A. Sommer. 1985. Energy Management of Chillers by Multilevel Control and Optimization. *Journal of Dynamic Systems, Measurement, and Control* **107**(4): 270-277.
Kloppers, J. C. and D. G. Kröger. 2005. The Lewis Factor and Its Influence on the Performance Prediction of Wet-Cooling Towers. *International Journal of Thermal Science* **44**(9): 879-884.
Kröger, D. G. 2004. *Air-Cooled Heat Exchangers and Cooling Towers - Thermal Flow Performance Evaluation and Design*. PennWell Corporation, Tulsa, OK.
Krstić, M. 2000. Performace Improvement and Limitations in Extremum Seeking Control. *Systems and Control Letters* **39**(5): 313-326.
Krstić, M. and H.-H. Wang. 2000. Stability of Extremum Seeking Feedback for General Nonlinear Dynamic Systems. *Automatica* **36**(4): 595-601.
Li, P., Y. Li and J. E. Seem. 2010. Efficient Operation of Air-Side Economizer Using Extremum Seeking Control. *Journal of Dynamic Systems, Measurement and Control* **132**(3): 031009 (10 pages).
Li, P., Y. Li and J. E. Seem. 2012. Consistent Initialazation of System of Differential-Algebraic Equations for Dynamic Simulation of Centrifugal Chillers. *Journal of Building Performance Simulation* **5**(2): 115-139.
Li, X., Y. Li and J. E. Seem. 2010. Dynamic Modeling of Mechanical Draft Counter-Flow Wet Cooling Tower with Modelica. *Proceedings of the 4th National Conference of IBPSA-USA*, 193-200, New York City, NY.
Liu, C.-W. and Y.-K. Chuah. 2011. A Study on an Optimal Approach Temperature Control Strategy of Condensing Water Temperature for Energy Saving. *International Journal of Refrigeration* **34**(3): 816-823.
Lu, L., W. Cai, Y. C. Soh, L. Xie and S. Li. 2004. HVAC System Optimization - Condenser Water Loop. *Energy Conversion and Management* **45**(4): 613-630.
Ma, Z., S. Wang, X. Xu and F. Xiao. 2008. A Supervisory Control Strategy for Building Cooling Water Systems for Practical and Real Time Applications. *Energy Conversion and Management* **49**(8): 2324-2336.
Modelica Association. 2012. *Modelica and Modelica Association*. From http://www.modelica.org/.
Poppe, M. and H. Rögener 1991. Berechnung von Rückkühlwerken, *VDI-Wärmeatlas*, Mi 1-Mi 15.
Richter, C. C. 2008. *Proposal of New Object-Oriented Model Libraries for Thermodynamic Systems*. Institute for Thermodynamics, Technical University at Braunschweig. **Ph. D. Thesis**.
Rotea, M. A. 2000. Analysis of Multivariable Extremum Seeking Algorithms. *Proceedings of American Control Conference*, 433-437. Chicago, IL.
Sane, H. S., C. Haugstetter and S. A. Bortoff. 2006. Building HVAC Control Systems - Role of Controls and Optimization. *Proceedings of American Control Conference*, 1121-1126, Minneapolis, Minnesota.
Sun, J. and A. Reddy. 2005. Optimal Control of Building HVAC&R Systems Using Complete Simulation-Based Sequential Quadratic Programming (CSB-SQP). *Building and Environment* **40**(5): 657-669.
TLK-Thermo GmbH. 2012. *Engineering Services and Software for Thermal Systems*. From: http://www.tlk-thermo.com/index.php.
Tyagi, V., H. Sane and S. Darbha. 2006. An Extremum Seeking Algorithm for Determining the Set Point Temperature for Condensed Water in a Cooling Tower. *ACC*, 1127-1131, Minneapolis, Minnesota.
U. S. Department of Energy. 2010. *Building Energy Data Book*, Technical Report.
Yao, Y., Z. Lian, Z. Hou and X. Zhou. 2004. Optimal Operation of a Large Cooling System Based on an Empirical Model. *Applied Thermal Engineering* **24**(16): 2303-2321.
Zhang, W., C. Zhang and G. Ding. 2009. Transient Modeling of an Air-Cooled Chiller with Economized Compressor. Part I: Model Development and Validation. *Applied Thermal Engineering* **29**: 2396-2402.